INTERNATIONAL JOURNAL FOR NUMERICAL METHODS IN FLUIDS
Int. J. Numer. Meth. Fluids 2009; **61**:683–697
Published online 23 December 2008 in Wiley InterScience (www.interscience.wiley.com). DOI: 10.1002/fld.1981

A higher-order accuracy lattice Boltzmann model for the wave equation

Jianying Zhang, Guangwu Yan*,† and Yinfeng Dong

Department of Mechanics and Engineering Mathematics, College of Mathematics, Jilin University, Changchun 130012, People's Republic of China

SUMMARY

A lattice Boltzmann model with higher-order accuracy for the wave motion is proposed. The new model is based on the technique of the higher-order moment of equilibrium distribution functions and a series of lattice Boltzmann equations in different time scales. The forms of moments are derived from the binary wave equation by designing the higher-order dissipation and dispersion terms. The numerical results agree well with classical ones. Copyright © 2008 John Wiley & Sons, Ltd.

Received 22 March 2008; Revised 31 October 2008; Accepted 8 November 2008

KEY WORDS: lattice Boltzmann model; higher-order moment; wave equation

1. INTRODUCTION

The lattice Boltzmann method (LBM) originated from a Boolean fluid model known as the lattice gas automata (LGA) [1] for modeling fluid flows. It has been developed as a new alternative method for computational fluid dynamics (CFD) [2]. The LBM starts from mesoscopic kinetic equation, i.e. the lattice Boltzmann equation, to determine macroscopic fluid flows. The kinetic nature brings certain advantages over conventional numerical methods, such as the algorithmic simplicity, parallel computation, easy handing of complex boundary conditions and efficient hydrodynamics simulations. During the past few years much progress has been made that extends the LBM as a tool for simulating many complex problems, such as multi-phase flow, suspensions flow and flow in porous media: flows that are quite difficult to simulate by conventional method [2–5]. On the other

*Correspondence to: Guangwu Yan, Department of Mechanics and Engineering Mathematics, College of Mathematics, Jilin University, Changchun 130012, People's Republic of China.
†E-mail: yangw@email.jlu.edu.cn

Contract/grant sponsor: Jilin University, National Nature Science Foundation of China; contract/grant numbers: 10072023, 90305013
Contract/grant sponsor: ChuangXin Foundation of Jilin University; contract/grant number: 2004CX041

hand, lattice Boltzmann model has undergone a number of further refinements. A new method, named as higher-order moment method, is proposed to obtain higher-order accuracy of truncation error. For example, recent studies by using this method show that the lattice Bhatnagar–Gross–Krook (LBGK) model could be used to simulate wave motion [6–8], the soliton wave [9], Lorenz attractor [10], and nonlinear Schrödinger equation [11, 12].

Now, we focus on the lattice Boltzmann model for the Wave equation [6–8, 13, 14]. The linear wave equation (LWE) governs the quantity $u(\mathbf{x},t)$ and

$$\frac{\partial^2 u}{\partial t^2}=a^2\frac{\partial^2 u}{\partial x^2}$$

where a is the wave speed. This equation can be transformed into the following form:

$$\begin{aligned}\frac{\partial u}{\partial t}+a\frac{\partial w}{\partial x}&=0\\ \frac{\partial w}{\partial t}+a\frac{\partial u}{\partial x}&=0\end{aligned} \tag{1}$$

where $u=u(\mathbf{x},t)$, $w=w(\mathbf{x},t)$ are real variables. We denote $u_1=u$, $u_2=w$, and introduce $A_{\sigma\beta}$ as

$$[A]=\begin{pmatrix}0 & a\\ a & 0\end{pmatrix}\equiv A_{\sigma\beta}$$

Equation (1) can be written as

$$\frac{\partial u_\sigma}{\partial t}+A_{\sigma\beta}\frac{\partial u_\beta}{\partial x}=0,\quad \sigma=1,2,\quad \beta=1,2 \tag{2}$$

where $\sigma=1$ and 2 refers to u and w parts, $\beta=1$ and 2 denotes the dimensions.

We have much interest in its lattice Boltzmann model with higher-order accuracy of truncation error. The lattice Boltzmann scheme has recently begun to receive considerable attention as an alternative numerical scheme for simulation of fluid flows and nonlinear systems. The conventional LBM, however, requires real one-particle distribution function. Because the wave equation (2) is scripted by two real quantities, the strategy we select to build lattice Boltzmann scheme is to separate the wave equation into two parts to obtain a two-species reaction–diffusion system [10]. This paper consists of three parts: (1) a series of lattice Boltzmann equations in different time scales and higher-order moment method are proposed, (2) a lattice Boltzmann model with higher-order accuracy for the wave equation is obtained, (3) numerical simulation examples are given.

In the next section, a series of lattice Boltzmann equations in different time scales and higher-order moment method are described. In Section 3, we contribute a lattice Boltzmann model with higher-order accuracy for the wave equation. In Section 4, we give two numerical examples, and Section 5 gives concluding remarks.

DOI: 10.1002/fld

2. A SERIES OF LATTICE BOLTZMANN EQUATIONS IN DIFFERENT TIME SCALES

2.1. *The lattice Boltzmann model*

We hold that the particles exist at a point in a probability with its mesoscopic velocity, and the quantities of particles evolve as the rule of lattice Boltzmann equation. In the process of evolution we assume that the distribution possesses equilibrium state. The following is the concrete details of the model in a way we used.

In D-dimensional space, the velocity of particles can be discretized into b directions, the particles move along the b links connecting each node and its nearest neighbors. In addition, there exist rest particles at each node, so the directions can be regarded as $b+1$ actually. Then if the process of colliding while particles are arriving at each node is considered additionally, the lattice Boltzmann equation will be obtained as

$$f_\alpha^\sigma(\mathbf{x}+\mathbf{e}_\alpha, t+1) = f_\alpha^\sigma(\mathbf{x}, t) - \frac{1}{\tau}[f_\alpha^\sigma(\mathbf{x}, t) - f_\alpha^{\sigma,\mathrm{eq}}(\mathbf{x}, t)] \tag{3}$$

where $f_\alpha^\sigma(\mathbf{x}, t)$ is the distribution function defined as the one-particle distribution function with species σ, velocity $\mathbf{e}_\alpha$ at time t, position $\mathbf{x}$. $f_\alpha^{\sigma,\mathrm{eq}}(\mathbf{x}, t)$ is the local equilibrium distribution, τ is the single-relaxation time factor. $f_\alpha^{\sigma,\mathrm{eq}}(\mathbf{x}, t)$ satisfies the conservation condition

$$\sum_\alpha f_\alpha^{\sigma,\mathrm{eq}}(\mathbf{x}, t) = \sum_\alpha f_\alpha^\sigma(\mathbf{x}, t) \tag{4}$$

2.2. *A series of lattice Boltzmann equations in different time scales*

We introduce the Knudsen number ε defined as $\varepsilon = \ell/L$ as the time step Δt [6], where ℓ is the mean free path and L is the characteristic length. Thus, the lattice Boltzmann equation (3) is changed into

$$f_\alpha^\sigma(\mathbf{x}+\varepsilon\mathbf{e}_\alpha, t+\varepsilon) = f_\alpha^\sigma(\mathbf{x}, t) - \frac{1}{\tau}[f_\alpha^\sigma(\mathbf{x}, t) - f_\alpha^{\sigma,\mathrm{eq}}(\mathbf{x}, t)] \tag{5}$$

In Equation (5), Knudsen number ε is assumed to be small, therefore, the Chapman–Enskog expansion [15] can be applied to $f_\alpha(\mathbf{x}, t)$. If the terms up to $O(\varepsilon^7)$ are retained, then

$$f_\alpha^\sigma = f_\alpha^{\sigma,\mathrm{eq}} + \sum_{n=1}^{6} \varepsilon^n f_\alpha^{\sigma,(n)} + O(\varepsilon^7) \tag{6}$$

Introducing different time scales $t_0, t_1, t_2, \ldots, t_6$ defined as

$$t_i = \varepsilon^i t, \quad i = 0, 1, \ldots, \tag{7}$$

thus,

$$\frac{\partial}{\partial t} = \sum_{i=0}^{i=6} \varepsilon^i \frac{\partial}{\partial t_i} + O(\varepsilon^7) \tag{8}$$

Using Taylor expansion in Equation (5), it is

$$f_\alpha^\sigma(\mathbf{x}+\varepsilon\mathbf{e}_\alpha, t+\varepsilon) - f_\alpha^\sigma(\mathbf{x}, t) = \sum_{n=1}^{6} \frac{\varepsilon^n}{n!} \left(\frac{\partial}{\partial t} + \mathbf{e}_\alpha \frac{\partial}{\partial \mathbf{x}}\right)^n f_\alpha^\sigma(\mathbf{x}, t) + O(\varepsilon^7) \tag{9}$$

DOI: 10.1002/fld

Combining Equations (5)–(9), the equation to the zero-order in ε is

$$\Delta f_\alpha^{\sigma,(0)} = -\frac{1}{\tau} f_\alpha^{\sigma,(1)} \tag{10}$$

where $f_\alpha^{\sigma,(0)} \equiv f_\alpha^{\sigma,\mathrm{eq}}$, partial differential operator $\Delta \equiv \partial/\partial t_0 + \mathbf{e}_\alpha \partial/\partial \mathbf{x}$.

Equations to other orders in ε are as follows:

$$\frac{\partial}{\partial t_1} f_\alpha^{\sigma,(0)} + \tau_2 \Delta^2 f_\alpha^{\sigma,(0)} = -\frac{1}{\tau} f_\alpha^{\sigma,(2)} \tag{11}$$

$$\tau_3 \Delta^3 f_\alpha^{\sigma,(0)} + 2\tau_2 \Delta \frac{\partial}{\partial t_1} f_\alpha^{\sigma,(0)} + \frac{\partial}{\partial t_2} f_\alpha^{\sigma,(0)} = -\frac{1}{\tau} f_\alpha^{\sigma,(3)} \tag{12}$$

$$\tau_4 \Delta^4 f_\alpha^{\sigma,(0)} + 3\tau_3 \Delta^2 \frac{\partial}{\partial t_1} f_\alpha^{\sigma,(0)} + 2\tau_2 \Delta \frac{\partial}{\partial t_2} f_\alpha^{\sigma,(0)} + \frac{\partial}{\partial t_3} f_\alpha^{\sigma,(0)} + \tau_2 \frac{\partial^2}{\partial t_1^2} f_\alpha^{\sigma,(0)} = -\frac{1}{\tau} f_\alpha^{\sigma,(4)} \tag{13}$$

$$\begin{aligned} &\tau_5 \Delta^5 f_\alpha^{\sigma,(0)} + 4\tau_4 \Delta^3 \frac{\partial}{\partial t_1} f_\alpha^{\sigma,(0)} + 3\tau_3 \Delta^2 \frac{\partial}{\partial t_2} f_\alpha^{\sigma,(0)} + 2\tau_2 \Delta \frac{\partial}{\partial t_3} f_\alpha^{\sigma,(0)} \\ &\quad + \frac{\partial}{\partial t_4} f_\alpha^{\sigma,(0)} + 3\tau_3 \Delta \frac{\partial^2}{\partial t_1^2} f_\alpha^{\sigma,(0)} + 2\tau_2 \frac{\partial^2}{\partial t_1 \partial t_2} f_\alpha^{\sigma,(0)} = -\frac{1}{\tau} f_\alpha^{\sigma,(5)} \end{aligned} \tag{14}$$

$$\begin{aligned} &\tau_6 \Delta^6 f_\alpha^{\sigma,(0)} + 5\tau_5 \Delta^4 \frac{\partial}{\partial t_1} f_\alpha^{\sigma,(0)} + 4\tau_4 \Delta^3 \frac{\partial}{\partial t_2} f_\alpha^{\sigma,(0)} + 3\tau_3 \Delta^2 \frac{\partial}{\partial t_3} f_\alpha^{\sigma,(0)} \\ &\quad + 2\tau_2 \Delta \frac{\partial}{\partial t_4} f_\alpha^{\sigma,(0)} + \frac{\partial}{\partial t_5} f_\alpha^{\sigma,(0)} + 6\tau_4 \Delta^2 \frac{\partial^2}{\partial t_1^2} f_\alpha^{\sigma,(0)} + 6\tau_3 \Delta \frac{\partial^2}{\partial t_1 \partial t_2} f_\alpha^{\sigma,(0)} \\ &\quad + 2\tau_2 \frac{\partial^2}{\partial t_1 \partial t_3} f_\alpha^{\sigma,(0)} + \tau_3 \frac{\partial^3}{\partial t_1^3} f_\alpha^{\sigma,(0)} + \tau_2 \frac{\partial^2}{\partial t_2^2} f_\alpha^{\sigma,(0)} = -\frac{1}{\tau} f_\alpha^{\sigma,(6)} \end{aligned} \tag{15}$$

In Equations (10)–(15) $\tau_1, \ldots, \tau_6$ are six polynomials of the relaxation time factor τ they are expressed as follows:

$$\tau_1 = 1 \tag{16}$$

$$\tau_2 = \tfrac{1}{2} - \tau \tag{17}$$

$$\tau_3 = \tau^2 - \tau + \tfrac{1}{6} \tag{18}$$

$$\tau_4 = -\tau^3 + \tfrac{3}{2}\tau^2 - \tfrac{7}{12}\tau + \tfrac{1}{24} \tag{19}$$

$$\tau_5 = \tau^4 - 2\tau^3 + \tfrac{5}{4}\tau^2 - \tfrac{1}{4}\tau + \tfrac{1}{120} \tag{20}$$

$$\tau_6 = -\tau^5 + \tfrac{5}{2}\tau^4 - \tfrac{13}{6}\tau^3 + \tfrac{3}{4}\tau^2 - \tfrac{31}{360}\tau + \tfrac{1}{720} \tag{21}$$

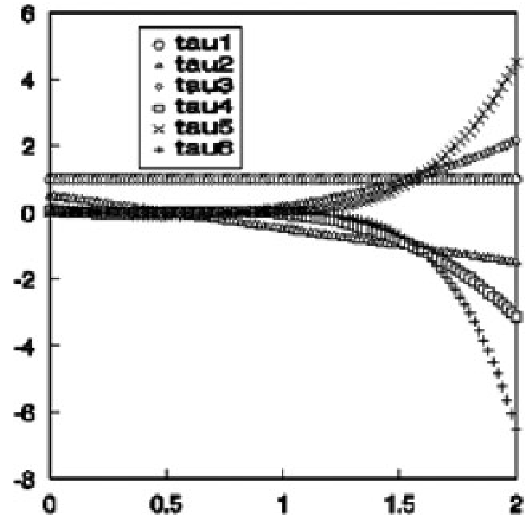

Figure 1. The relations between coefficients τ_i and τ. tau1, tau2, ..., tau6 represent $\tau_1, \ldots, \tau_6$, respectively.

These polynomials (16)–(21) have the character: when $\tau > 1.0$, τ_2, τ_4 and τ_6 are negative numbers, but τ_3 and τ_5 are positive numbers. In Figure 1, we plot the relations between τ_i and the relaxation time factor τ.

Equations (10)–(15) is so-called a series of lattice Boltzmann equations in different time scales. It is suitable for one-, two- and three-dimensional case. In Reference [6] four lattice Boltzmann equations (10)–(13) are given. Nevertheless, it is not enough to find equations with higher-order accuracy. By adding lattice Boltzmann equations (14)–(15), the wave equation with more than two-order accuracy could be obtained.

2.3. *Equilibrium distribution functions and their higher-order moments*

The macroscopic quantity $u_\sigma(\mathbf{x}, t)$ in one-dimensional wave equation (2) is defined by

$$u_\sigma(\mathbf{x}, t) = \sum_\alpha f_\alpha^\sigma(\mathbf{x}, t) \tag{22}$$

According to the conservation condition (4), we have

$$\sum_\alpha f_\alpha^{\sigma,\mathrm{eq}}(\mathbf{x}, t) = u_\sigma(\mathbf{x}, t) \tag{23}$$

and

$$\sum_\alpha f_\alpha^{\sigma,(n)}(\mathbf{x}, t) = 0, \quad n \geqslant 1 \tag{24}$$

The moments of equilibrium distribution function are defined as

$$u_\sigma(\mathbf{x}, t) = \sum_\alpha f_\alpha^{\sigma,(0)}(\mathbf{x}, t) \tag{25}$$

$$m_\sigma^0(\mathbf{x}, t) = \sum_\alpha f_\alpha^{\sigma,(0)}(\mathbf{x}, t) e_\alpha \tag{26}$$

DOI: 10.1002/fld

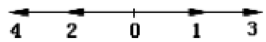

Figure 2. Diagrammatic sketch of one-dimensional 5-bit lattice.

$$\pi_\sigma^0(\mathbf{x}, t) = \sum_\alpha f_\alpha^{\sigma,(0)}(\mathbf{x}, t) e_\alpha^2 \tag{27}$$

$$P_\sigma^0(\mathbf{x}, t) = \sum_\alpha f_\alpha^{\sigma,(0)}(\mathbf{x}, t) e_\alpha^3 \tag{28}$$

$$Q_\sigma^0(\mathbf{x}, t) = \sum_\alpha f_\alpha^{\sigma,(0)}(\mathbf{x}, t) e_\alpha^4 \tag{29}$$

$$R_\sigma^0(\mathbf{x}, t) = \sum_\alpha f_\alpha^{\sigma,(0)}(\mathbf{x}, t) e_\alpha^5 \tag{30}$$

$$S_\sigma^0(\mathbf{x}, t) = \sum_\alpha f_\alpha^{\sigma,(0)}(\mathbf{x}, t) e_\alpha^6 \tag{31}$$

Let us consider a 5-bit model, the discrete velocities set is $e_\alpha = (0, c, -c, 2c, -2c)$, where $\alpha = 0, 1, \ldots, 4$, c is the magnitude of velocity. The diagrammatic sketch of lattice is shown as Figure 2.

The equilibrium distribution functions of 5-bit model can be solved by Equations (25)–(29), they are

$$f_1^{\sigma,(0)} = \frac{1}{6c^4}(4m_\sigma^0 c^3 + 4\pi_\sigma^0 c^2 - Q_\sigma^0 - P_\sigma^0 c) \tag{32}$$

$$f_2^{\sigma,(0)} = \frac{1}{6c^4}(-4m_\sigma^0 c^3 + 4\pi_\sigma^0 c^2 - Q_\sigma^0 + P_\sigma^0 c) \tag{33}$$

$$f_3^{\sigma,(0)} = \frac{1}{24c^4}(2P_\sigma^0 c - 2m_\sigma^0 c^3 + Q_\sigma^0 - \pi_\sigma^0 c^2) \tag{34}$$

$$f_4^{\sigma,(0)} = \frac{1}{24c^4}(-2P_\sigma^0 c + 2m_\sigma^0 c^3 + Q_\sigma^0 - \pi_\sigma^0 c^2) \tag{35}$$

$$f_0^{\sigma,(0)} = u_\sigma - f_1^{\sigma,(0)} - f_2^{\sigma,(0)} - f_3^{\sigma,(0)} - f_4^{\sigma,(0)} \tag{36}$$

When these moments are determined, the equilibrium distribution functions will be found.

3. LATTICE BOLTZMANN MODEL FOR THE BINARY WAVE EQUATIONS

Making $(10) + (11) * \varepsilon + (12) * \varepsilon^2 + (13) * \varepsilon^3 + (14) * \varepsilon^4$ and summing Equations (10)–(14) over α, we have

$$\frac{\partial u_\sigma}{\partial t} + A_{\sigma\beta}\frac{\partial u_\beta}{\partial x} + E_1 + E_2 + E_3 + E_4 = O(\varepsilon^5) \tag{37}$$

In Equation (37),

$$E_1 = \varepsilon \sum_\alpha \tau_2 \Delta^2 f_\alpha^{\sigma,(0)} \tag{38}$$

$$E_2 = \varepsilon^2 \sum_\alpha \left(\tau_3 \Delta^3 f_\alpha^{\sigma,(0)} + 2\tau_2 \Delta \frac{\partial}{\partial t_1} f_\alpha^{\sigma,(0)} \right) \tag{39}$$

$$E_3 = \varepsilon^3 \sum_\alpha \left(\tau_4 \Delta^4 f_\alpha^{\sigma,(0)} + 3\tau_3 \Delta^2 \frac{\partial}{\partial t_1} f_\alpha^{\sigma,(0)} + 2\tau_2 \Delta \frac{\partial}{\partial t_2} f_\alpha^{\sigma,(0)} + \tau_2 \frac{\partial^2}{\partial t_1^2} f_\alpha^{\sigma,(0)} \right) \tag{40}$$

$$E_4 = \varepsilon^4 \sum_\alpha \left(\tau_5 \Delta^5 f_\alpha^{\sigma,(0)} + 4\tau_4 \Delta^3 \frac{\partial}{\partial t_1} f_\alpha^{\sigma,(0)} + 3\tau_3 \Delta^2 \frac{\partial}{\partial t_2} f_\alpha^{\sigma,(0)} + 2\tau_2 \Delta^2 \frac{\partial}{\partial t_3} f_\alpha^{\sigma,(0)} \right.$$
$$\left. + 3\tau_3 \Delta \frac{\partial^2}{\partial t_1^2} f_\alpha^{\sigma,(0)} + 2\tau_2 \frac{\partial^2}{\partial t_1 \partial t_2} f_\alpha^{\sigma,(0)} \right) \tag{41}$$

Summing Equation (10) over α, we obtain the conservation law in time scale t_0

$$\frac{\partial u_\sigma}{\partial t_0} + \frac{\partial m_\sigma^0}{\partial x} = 0 \tag{42}$$

In order to find those E_1, E_2, E_3 and E_4, we assume that moments satisfy

$$m_\sigma^0(\mathbf{x}, t) = \sum_\alpha f_\alpha^{\sigma,(0)}(\mathbf{x}, t) e_\alpha = A_{\sigma\beta} u_\beta \tag{43}$$

$$\pi_\sigma^0(\mathbf{x}, t) = \sum_\alpha f_\alpha^{\sigma,(0)}(\mathbf{x}, t) e_\alpha^2 = A_{\sigma\beta} A_{\beta\gamma} u_\gamma \tag{44}$$

$$P_\sigma^0(\mathbf{x}, t) = \sum_\alpha f_\alpha^{\sigma,(0)}(\mathbf{x}, t) e_\alpha^3 = A_{\sigma\beta} A_{\beta\gamma} A_{\gamma\delta} u_\delta - \Gamma u_\sigma \tag{45}$$

$$Q_\sigma^0(x, t) = \sum_\alpha f_\alpha^{\sigma,(0)}(\mathbf{x}, t) e_\alpha^4 = A_{\sigma\beta} A_{\beta\gamma} A_{\gamma\delta} A_{\delta\eta} u_\eta - K u_\sigma - \Gamma A_{\sigma\beta} u_\beta \tag{46}$$

where Γ, K are parameters. According to Equations (32)–(36), these equilibrium distribution functions $f_\alpha^{\sigma,(0)}$ can be found, and the moment R_σ^0 is determined

$$R_\sigma^0 = \sum_\alpha f_\alpha^{\sigma,(0)} e_\alpha^5 = (f_1^{\sigma,(0)} - f_2^{\sigma,(0)}) c^5 + 32 (f_3^{\sigma,(0)} - f_4^{\sigma,(0)}) c^5$$
$$= 5 P_\sigma^0 c^2 - 4 m_\sigma^0 c^4 \tag{47}$$
$$= 5c^2 A_{\sigma\beta} A_{\beta\gamma} A_{\gamma\delta} u_\delta - 4c^4 A_{\sigma\beta} u_\beta$$

DOI: 10.1002/fld

If we set $\Gamma=0$, therefore

$$E_1=\varepsilon\sum_\alpha \tau_2\Delta^2 f_\alpha^{\sigma,(0)}=\varepsilon\tau_2\left[\frac{\partial}{\partial t_0}\left(\frac{\partial u_\sigma}{\partial t_0}+\frac{\partial m_\sigma^0}{\partial x}\right)+\frac{\partial}{\partial x}\left(\frac{\partial m_\sigma^0}{\partial t_0}+\frac{\partial \pi_\sigma^0}{\partial x}\right)\right]=0 \tag{48}$$

$$E_2=\varepsilon^2\sum_\alpha\left(\tau_3\Delta^3 f_\alpha^{\sigma,(0)}+2\tau_2\Delta\frac{\partial}{\partial t_1}f_\alpha^{\sigma,(0)}\right)=\varepsilon^2\tau_3\sum_\alpha\Delta^3 f_\alpha^{\sigma,(0)}=0 \tag{49}$$

$$\begin{aligned}E_3&=\varepsilon^3\sum_\alpha\left(\tau_4\Delta^4 f_\alpha^{\sigma,(0)}+3\tau_3\Delta^2\frac{\partial}{\partial t_1}f_\alpha^{\sigma,(0)}+2\tau_2\Delta\frac{\partial}{\partial t_2}f_\alpha^{\sigma,(0)}+\tau_2\frac{\partial^2}{\partial t_1^2}f_\alpha^{\sigma,(0)}\right)\\&=-\varepsilon^3\tau_4 K\frac{\partial^4 u_\sigma}{\partial x^4}\end{aligned} \tag{50}$$

$$\begin{aligned}E_4&=\tau_5\varepsilon^4\sum_\alpha\left[4\frac{\partial^4}{\partial t_0\partial x^3}\left(\frac{\partial P_\sigma^0}{\partial t_0}+\frac{\partial Q_\sigma^0}{\partial x}\right)+\frac{\partial^4}{\partial x^4}\left(\frac{\partial Q_\sigma^0}{\partial t_0}+\frac{\partial R_\sigma^0}{\partial x}\right)\right]\\&=\tau_5\varepsilon^4[(5K-4c^4)A_{\sigma\beta}\delta_{\beta\xi}-A_{\sigma\beta}A_{\beta\gamma}A_{\gamma\delta}A_{\delta\eta}A_{\eta\xi}+5c^2A_{\sigma\beta}A_{\beta\gamma}A_{\gamma\delta}\delta_{\delta\xi}]\frac{\partial^5 u_\xi}{\partial x^5}\end{aligned} \tag{51}$$

Equation (37) is

$$\frac{\partial u_\sigma}{\partial t}+A_{\sigma\beta}\frac{\partial u_\beta}{\partial x}=\varepsilon^3\tau_4 K\frac{\partial^4 u_\sigma}{\partial x^4}-E_4+O(\varepsilon^5) \tag{52}$$

The truncation error is

$$R=-\varepsilon^3\tau_4 K\frac{\partial^4 u_\sigma}{\partial x^4}+E_4+O(\varepsilon^5) \tag{53}$$

Selecting the parameter $K=0$, Equation (37) becomes

$$\frac{\partial u_\sigma}{\partial t}+A_{\sigma\beta}\frac{\partial u_\beta}{\partial x}=O(\varepsilon^4) \tag{54}$$

The stability of the lattice Boltzmann scheme Equation (5) is controlled by the coefficient of the term $\partial^4 u_\sigma/\partial x^4$ whether negative or not [16]. If the lattice Boltzmann scheme is stable, $\varepsilon^3\tau_4 K$ has to be negative, if $K>0$, $\tau>1$ then $\tau_4<0$, $K\varepsilon^3\tau_4<0$. In this paper, $\tau=1.2$, $K=1$, $\tau_4=-0.22633339$.

4. NUMERICAL EXAMPLES

To test the effect of this model, we choose two examples for one-dimensional wave equation. We select the lattice size M, the mesoscopic speed c, the step of x as Δx. The length of the computing region is $l=M\Delta x$; the Knudsen number is $\varepsilon=\Delta x/c$. The wave propagation speed is a. The initial condition of distribution function is given by Equations (32)–(36) from the macroscopic quantity u_σ at time $t=0$. The boundary conditions of f_α^σ are given by Equations (32)–(36) from the macroscopic quantity u_σ on boundaries.

Example 1

The one-dimensional wave equation is

$$\begin{cases} \dfrac{\partial^2 u}{\partial t^2} = a^2 \dfrac{\partial^2 u}{\partial x^2}, \quad t>0, \quad -\infty<x<\infty \\ u(x,0) = \dfrac{0.2}{1+9x^2}, \quad \dfrac{\partial u(x,0)}{\partial t} = 0 \end{cases} \tag{55}$$

This problem has exact solution [6]

$$u_e(x,t) = \frac{0.1}{1+9(x-at)^2} + \frac{0.1}{1-9(x-at)^2} \tag{56}$$

where a is the wave propagation speed.

In this example, the computing region is $[-5,5]$, the wave propagation speed $a=0.1$, lattice size $M=1000$, $\Delta x = 0.01$, $c=3.0$, thus, $\varepsilon = \Delta t = \Delta x / c = \frac{1}{3} \times 10^{-2}$, $\tau = 1.2$, $K=1.0$. In Figure 3, we plot curves at the time steps $N=2000$, 6000 and 8000. The boundary conditions are $\partial u(-5,t)/\partial x = 0$ and $\partial u(5,t)/\partial x = 0$.

In Figure 3(a–d), we plot the wave motion at three moments besides initial condition. We find that the single wave packet evolves into a right-traveling wave packet and a left-traveling wave packet and the shapes are preserved at all times. We also give the errors by using function $e(x,t) = |(u(x,t) - u_e(x,t))/u_e(x,t)|$, where $u_e(x,t)$ is the exact solution in Equation (56). In Figure 3(e), we plot the curve of errors versus position x. By comparison, this result has higher accuracy than the result in Reference [6] since it has the fourth-order accuracy of truncation error. The relative error is around the scope of $(-1.0 \times 10^{-4}, 1.0 \times 10^{-4})$. This numerical result shows good agreement with exact solution.

Example 2

Consider wave equations:

$$\frac{\partial u_\sigma}{\partial t} + A_{\sigma\beta} \frac{\partial u_\beta}{\partial x} = 0, \quad \sigma = 1,2, \quad \beta = 1,2, \quad A = \begin{pmatrix} 0 & 1 \\ 1 & 0 \end{pmatrix} \tag{57}$$

with square wave initial condition

$$u_1^0(x) = \begin{cases} 1, & -2 \leqslant x \leqslant -1 \\ 0 & \text{others} \end{cases} \tag{58}$$

$$u_2^0(x) = \begin{cases} 1, & 1 \leqslant x \leqslant 2 \\ 0 & \text{others} \end{cases} \tag{59}$$

It possesses the exact solution [16–18]

$$u_1(x,t) = \tfrac{1}{2}[u_1^0(x-t) + u_1^0(x+t)] + \tfrac{1}{2}[u_2^0(x-t) - u_2^0(x+t)] \tag{60}$$

$$u_2(x,t) = \tfrac{1}{2}[u_2^0(x-t) + u_2^0(x+t)] + \tfrac{1}{2}[u_1^0(x-t) - u_1^0(x+t)] \tag{61}$$

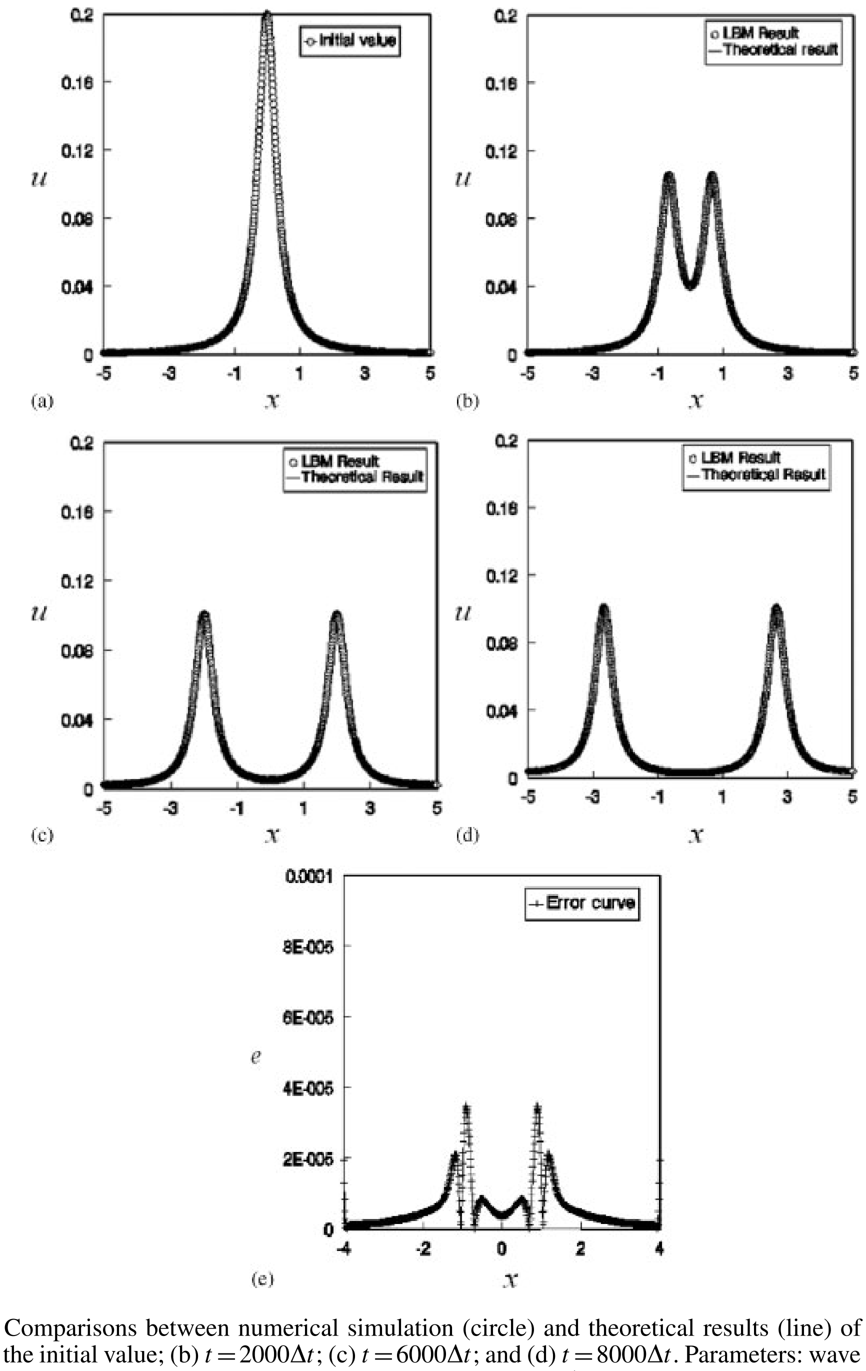

Figure 3. Comparisons between numerical simulation (circle) and theoretical results (line) of Example 1, where (a) the initial value; (b) $t=2000\Delta t$; (c) $t=6000\Delta t$; and (d) $t=8000\Delta t$. Parameters: wave propagation speed $a=0.1$, lattice size $M=1000$, $\Delta x=0.01$, $c=3.0$, $\varepsilon=\Delta t=\frac{1}{3}\times 10^{-2}$, $\tau=1.2$, $K=1.0$. (e) The errors curve versus position x at time $t=3000\Delta t$.

DOI: 10.1002/fld

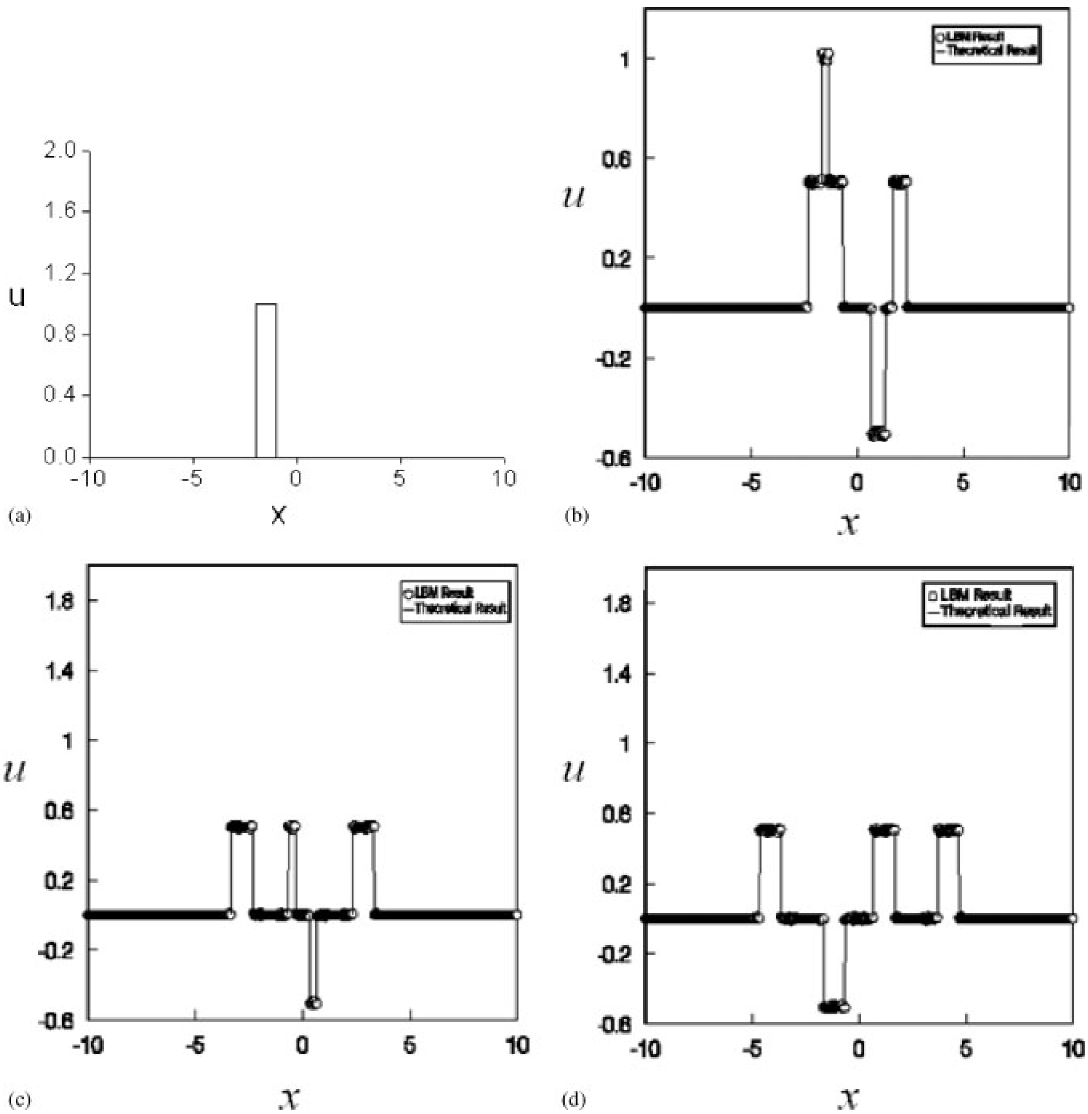

Figure 4. Comparisons between numerical simulation (circle) and theoretical results (line) of the macroscopic quantity u for Example 2, where (a) the initial value; (b) $t=100\Delta t$; (c) $t=400\Delta t$; and (d) $t=800\Delta t$. Computing region is $[-10, 10]$, lattice size $M=2000$, $\Delta x=0.01$, $c=3$, $\varepsilon=\Delta t=\frac{1}{3}\times 10^{-2}$, $\tau=1.2$, $K=1.0$.

In this example, the computing region is $[-10, 10]$, lattice size $M=2000$, $\Delta x=0.01$, $c=3.0$, thus, $\varepsilon=\Delta t=\Delta x/c=\frac{1}{3}\times 10^{-2}$, $\tau=1.2$, $K=1.0$. The boundary conditions are $\partial u_\sigma(-10,t)/\partial x=0$ and $\partial u_\sigma(10,t)/\partial x=0$, $\sigma=1,2$.

In Figure 4(a–d), we plot the comparisons between numerical simulation (circle) and theoretical results (line) of the wave motion of macroscopic quantity $u(x,t)$ at four moments for Example 2, (a) $t=0$, (b) $t=100\Delta t$, (c) $t=400\Delta t$, (d) $t=800\Delta t$. At initial time, a square wave $u(x,t)$ was

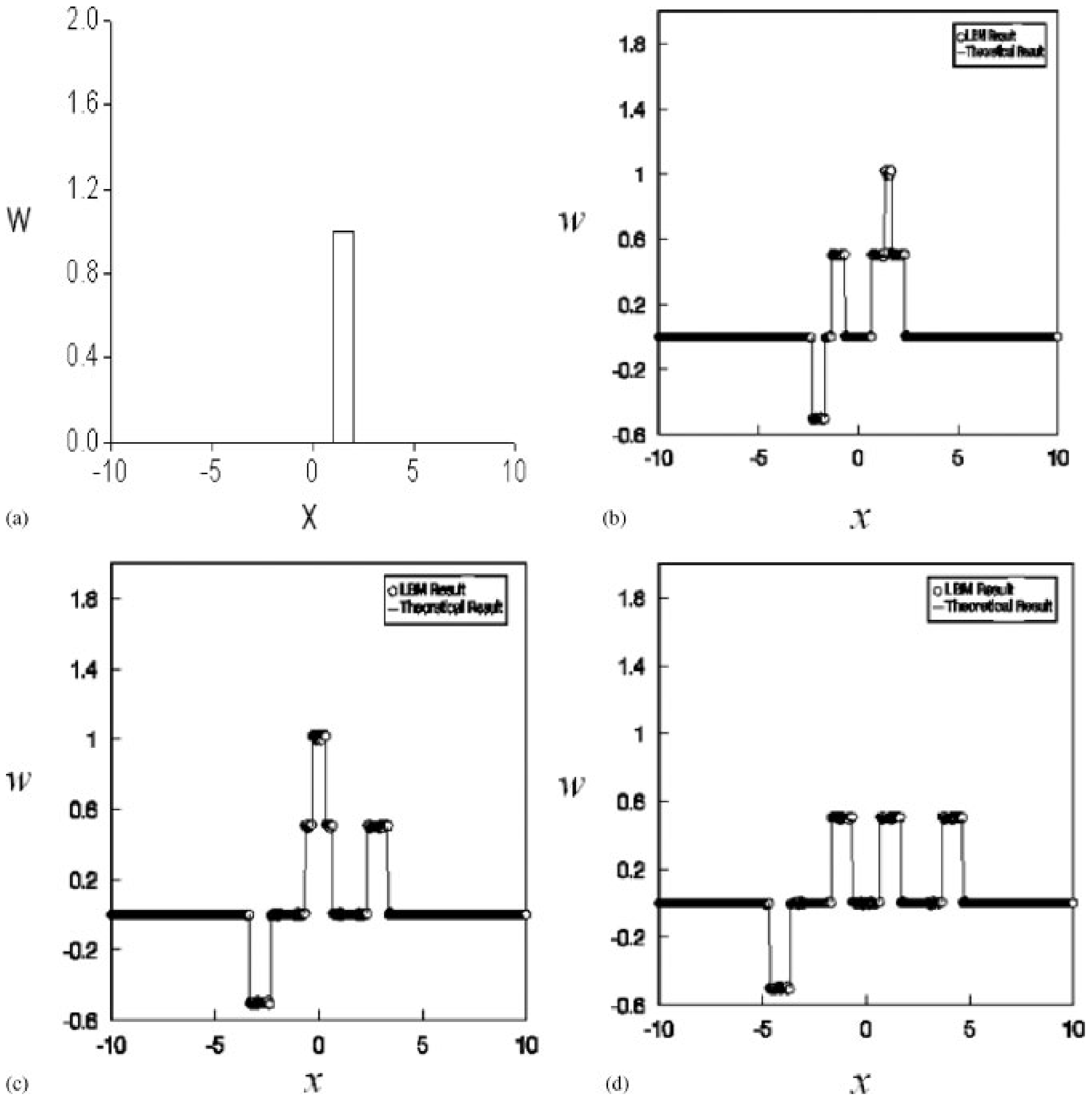

Figure 5. Comparisons between numerical simulation (circle) and theoretical results (line) of the macroscopic quantity w for Example 2, where (a) the initial value; (b) $t=100\Delta t$; (c) $t=400\Delta t$; and (d) $t=800\Delta t$. Computing region is $[-10, 10]$, lattice size $M=2000$, $\Delta x=0.01$, $c=3$, $\varepsilon=\Delta t=\frac{1}{3}\times 10^{-2}$, $\tau=1.2$, $K=1.0$.

placed at plane x–u. We find that another square wave emerges immediately due to quantity $w(x,t)$, and then per square wave packet evolves into a right-traveling square wave and a left-traveling square wave packet. The two kinds of square wave packets will meet and collide and then they will pass through each other. This numerical result shows good agreement with exact solution. Figure 5(a–d) shows the wave motion of macroscopic quantity $w(x,t)$ at four moments, (a) $t=0$, (b) $t=100\Delta t$, (c) $t=400\Delta t$, (d) $t=800\Delta t$.

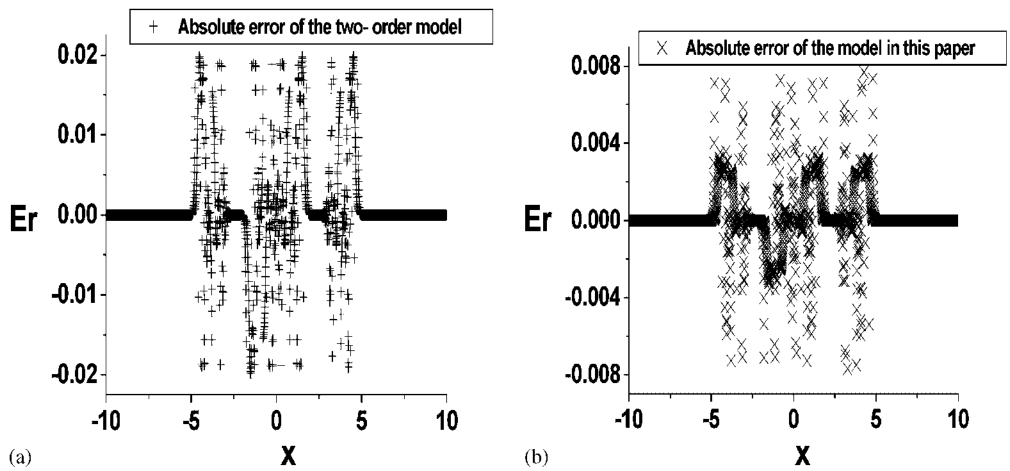

Figure 6. Absolute errors of the macroscopic quantity u at $t=800\Delta t$ for Example 2, where (a) the result of two-order model in Reference [6]; (b) the result of two-order model in this paper. Computing region is $[-10, 10]$, lattice size $M=2000$, $\Delta x=0.01$, $c=3$, $\varepsilon=\Delta t=\frac{1}{3}\times 10^{-2}$, $\tau=1.2$, $K=1.0$.

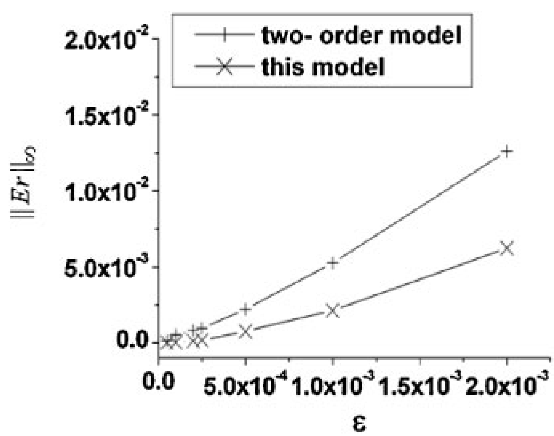

Figure 7. The curves of the infinite norm of the absolute error $\mathrm{Er}=u-u^*$ versus the Knudsen number ε to Example 2. The parameters are: $c=3.0$, time $t=2.0$, $\tau=1.2$, $K=1.0$. The space region is $x\in[-10, 10]$.

In Figure 6, we give the absolute errors of the macroscopic quantity u at $t=800\Delta t$ for Example 2, where (a) the result of two-order model in Reference [6]; (b) the result of two-order model in this paper. From the comparison in (a) and (b), the absolute error of the LBM was found to be smaller than the absolute error of the two-order LBM in Reference [6]. It is in good agreement with exact solution. From the absolute errors of the two LBM results and exact solution in (b), we could see the errors of the LBM results within a region of $(-0.008, 0.008)$.

We also plot the curves of the infinite norm of the absolute error $\mathrm{Er}=u-u^*$ versus the Knudsen number ε at $t=2.0$ to Example 2, where u^* is the exact solution, see Figure 7. This figure shows

DOI: 10.1002/fld

the relations between the absolute error and the Knudsen number ε. It provides a qualitative trend of the numerical order of convergence. We also find the absolute error of the LBM is smaller than the absolute error of the two-order LBM in Reference [6].

5. CONCLUDING REMARKS

In this paper, a lattice Boltzmann model for wave equation with higher-order accuracy is proposed. A key step is that a series of lattice Boltzmann equations in different time scales is given; therefore, the equilibrium distribution functions of one-dimensional case are expressed by moments of them.

In order to improve the order of truncation errors, we add more terms of higher power of u. When the higher-order moments are determined, the equilibrium distribution functions are known. In this paper a 5-bit model is used; thus, five moments are proposed.

Finally we point out that this method and the main idea in the paper, including a series of partial differential equations in different time scales and its equilibrium distribution, can be spread into two- and three-dimensional linear and nonlinear wave equation. Nevertheless, there are many problems to be solved to develop this model as a tool of simulating linear and nonlinear wave equation. We would discuss these problems in further papers.

ACKNOWLEDGEMENTS

This work is supported by the 985 Project of Jilin University, the National Nature Science Foundation of China (Grant nos. 10072023, 90305013), and the ChuangXin Foundation of Jilin University (No. 2004CX041). We would like to thank Prof. Hu Shouxin, Prof. Wang Jianping, and Liu Yanhong, Shi Xiubo, Wang Huimin, and Yan Bo for their many helpful suggestions.

REFERENCES

1. Frisch U, Hasslacher B, Pomeau Y. Lattice gas automata for the Navier–Stokes equations. *Physical Review Letters* 1986; **56**:1505–1508.
2. Chen SY, Doolen GD. Lattice Boltzmann method for fluid flows. *Annual Fluid Mechanics* 1998; **3**:314–322.
3. Qian YH, d'Humieres D, Lallemand P. Lattice BGK model for Navier–Stokes equations. *Europhysics Letters* 1992; **17**(6):479–484.
4. Chen HD, Chen SY, Matthaeus MH. Recovery of the Navier–Stokes equations using a lattice Boltzmann gas method. *Physical Review A* 1992; **45**:5339–5342.
5. Benzi R, Succi S, Vergassola M. The lattice Boltzmann equations: theory and applications. *Physics Reports* 1992; **222**:147–197.
6. Yan GW. A lattice Boltzmann equation for waves. *Journal of Computational Physics* 2000; **161**:61–69.
7. Wang MR, Wang JK, Chen SY. Roughness and cavitations effects on electro-osmotic flows in rough microchannels using the lattice Poisson–Boltzmann methods. *Journal of Computational Physics* 2007; **226**:836–851.
8. Wang MR, Chen SY. Electroosmosis in homogeneously charged micro- and nanoscale random porous media. *Journal of Colloid and Interface Science* 2007; **314**:264–273.
9. Yan GW, Song M. Recovery of the solitons using a lattice Boltzmann model. *Chinese Physics Letters* 1999; **16**:109–110.
10. Yan GW, Yuan L. Lattice Bhatnagar–Gross–Krook model for the lorenz attractor. *Physica D* 2001; **154**:43–50.
11. Succi S. Lattice Boltzmann mechanics, an application to Bose–Einstein condensation. *International Journal of Modern Physics C* 1998; **9**:1577–1585.
12. Zhang JY, Yan GW. A lattice Boltzmann model for the nonlinear Schrödinger equation. *Journal of Physics A* 2007; **40**:10393–10405.
13. Chen HD, Chen SY, Doolen G, Lee YC. Simple lattice gas models for wave. *System 2* 1988; **2**:259–267.

14. Wolf-Gladrow DA. *Lattice-Gas Cellular Automata and Lattice Boltzmann Models*: *An Introduction*. Springer: Berlin, 2000.
15. Chapman S, Cowling TG. *The Mathematical Theory of Non-uniform Gas*. Cambridge University Press: Cambridge, 1970.
16. Liu RX, Shu CW. *Some New Methods on Computation Fluid Dynamics*. Science Press: Beijing, 2003 (in Chinese).
17. Taniuti T, Nishihara K. *Nonlinear Waves*. Pitman Advanced Publishing Program: Boston, 1983.
18. Whitham GB. *Linear and Nonlinear Waves*. Wiley: New York, 1974.